Ab Initio Quantum Mechanical and Molecular Dynamical Study of Intra- and Intermolecular Anhydride Formation

Mikael Peräkylä

Department of Chemistry, University of Kuopio, P.O. Box 1627, FIN-70211, Kuopio, Finland

Peter A. Kollman*

Department of Pharmaceutical Chemistry, University of California, San Francisco, California 94143-0446

Received: February 22, 1999; In Final Form: July 7, 1999

Ab initio quantum mechanical gas phase (MP2/6-31+G*//HF/6-31G*), continuum solvation model (IPCM-HF/6-31G*), and molecular dynamical potential of mean force calculations were used to study the intermolecular anhydride formation reaction between acetate and acetate phenyl ester (**1**), and the corresponding intramolecular reaction of glutarate (**2**), succinate (**3**), and 3,6-endoxo-Δ^4-tetrahydrophthalate monoester (**4**). Energies were calculated for the two sequential steps of the reaction: (1) the formation of a reactive bimolecular ion−molecule complex from the separated reactants (**1**) or intramolecular ion−molecule complex from a pool of extended conformations (**2**−**4**) and (2) the formation of transition state from the ion−molecule complex. The calculated reaction activation energies in aqueous solution correlated very well with the experimental values. The differences in the gas-phase energies, solvation energies, and the free energy cost to bring the separated reactants together in a bimolecular ion−molecule complex (for intermolecular reaction) were all found to be important in explaining the reactivity differences of the molecules studied. In addition, both steps contributed to the reactivity differences.

Introduction

Studies of enzyme models have often revealed how the remarkable selectivity and efficiency in enzyme-catalyzed reactions, compared to the corresponding noncatalyzed reactions, are accomplished.[1−4] These studies have provided information on how different structural and environmental variables such as enforced geometric disposition of the reacting functional groups in a suitable geometry, increased rigidity and strain in the structure of the model system and solvation affect the reaction rate and selectivity. Although the general factors playing important roles in regulating the reactivities in general are well characterized, the quantitative role of the factors in specific cases is often unclear.

Intramolecular anhydride formation by substituted monoesters has often been used as a textbook example of proximity and entropy effects in intramolecular and enzymatic reactions (see reaction 1).[5]

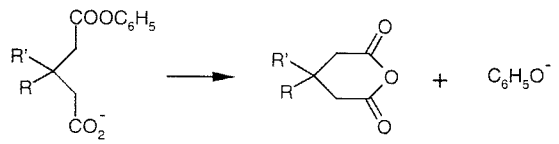

In this reaction the enhancement of the intramolecular reaction is 10^8 faster than that of the corresponding intermolecular reaction.[2,3] Over the years several explanations have been given for the rate acceleration observed in intramolecular reactions. It is obvious that a significant part of the rate enhancement of changing an intermolecular reaction to an intramolecular one can be attributed to a decrease in translational and rotational entropy.[6] By analogy, a significant part of the catalytic efficiency of enzyme reactions seems to be due to the preorganization of the catalytic groups and substrate in the enzyme−substrate complex.[7] Further increases in the rates of intramolecular reactions have been suggested to arise from (i) the removal of translational and rotational degrees of freedom,[6,8] (ii) the probability of formation of a reactive conformer,[5] and (iii) solvation effects.[4] Recently Lightstone and Bruice[5,9] have studied intramolecular ester hydrolysis of substituted monoesters computationally. They concluded that changes in rate constants are due to the ground-state phenomena and are related to the ease by which a near-attack conformation (NAC) is formed from a pool of extended conformations. A NAC was defined to be a conformation in which the distance of approach of the nucleophilic oxygen to the carbonyl carbon is 2.8−3.2 Å, and the oxygen approaches the carbonyl group at an attack angle of 75 ± 15°.[5] Thus, the orbitals of the reacting groups are properly aligned in a pretransition state where they are ready to initiate the reaction.

In this work we have used ab initio quantum mechanical and molecular dynamical methods to study the intermolecular anhydride formation reaction between acetate and acetate phenyl ester (**1**), and the corresponding intramolecular reaction of glutarate (**2**), succinate (**3**), and 3,6-endoxo-Δ^4-tetrahydrophthalate monoester (**4**, Chart 1) in the gas phase and in aqueous solution. In this series of compounds the enhancement of the reaction rate achieved by fixing the reacting groups in a conformation resembling the transition state is 10^8.[2,3] The transition state energies calculated in this work for the anhydride formation reaction correlate well with the experiments, allowing us to use the computed results in explaining the factors which determine the differences in the reactivities of the molecules.

10.1021/jp990619r CCC: $18.00
Published on Web 09/23/1999

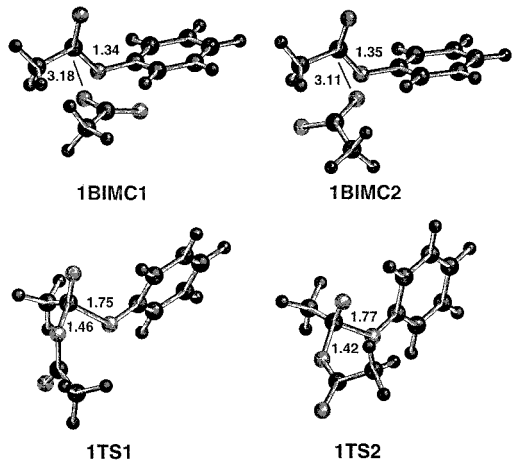

Figure 1. Structures and selected bond distances (in angstroms) of 1BIMC1, 1BIMC2, 1TS1, and 1TS2.

CHART 1

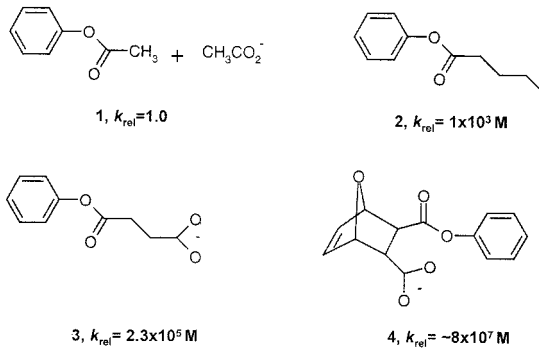

Computational Details

Calculation of Reaction Energies. The reaction mechanism of the anhydride formation reaction is divided here into two sequential steps (eq 2): (1) the formation of a bimolecular ion−molecule complex (Figure 1, BIMC, for **1**) from separated reactants or intramolecular ion−molecule complex (Figures 2−4, IIMC, for **2**−**4**) from a pool of extended conformations and (2) the step from BIMC/IIMC to the transition state (TS, Figures 1−4) of the reaction.

(2) separated reactants/extended

$$\text{conformations} \xleftrightarrow{\text{step 1}} \text{BIMCs/IIMCs} \xleftrightarrow{\text{step 2}} \text{TS}$$

In this work the reactive bimolecular (BIMC, for **1**) and intramolecular ion−molecule complexes (IIMC, for **2**−**4**) were defined to be conformations in which the nucleophilic oxygen was suitably positioned (distance less than 3.2 Å and favorable attack angle 75 ± 15°) to attack the ester carbonyl. BIMC/IIMC formation free energies (ΔG_{IMC}(IPCM) and ΔG_{IMC}(MD), step 1) were calculated with the Boltzman equation (eq 3).

$$\Delta G_{IMC} = -RT \ln \frac{\sum_{IMC} e^{-\Delta E_{IMC}/RT}}{\sum_{EXT} e^{-\Delta E_{EXT}/RT}}$$

In eq 3, the subscript IMC refers to the reactive ion−molecule complexes and subscript EXT to the rest of the conformations found in the conformational analysis. Relative aqueous phase (free) energies used in eq 3 for the different conformations were calculated from the relative gas-phase (ΔE_{gas}) energies, and solvation energies of the species from continuum solvation calculations ($\Delta\Delta G_{solv}$(IPCM), eq 4a) or molecular dynamical potential of mean force calculations ($\Delta\Delta G_{solv}$(MD), eq 4b).

$$\text{(4a)}\ \Delta E_{sol}(\text{IPCM}) = \Delta E_{gas} + \Delta\Delta G_{solv}(\text{IPCM})$$

$$\text{(4b)}\ \Delta E_{sol}(\text{MD}) = \Delta E_{gas} + \Delta\Delta G_{solv}(\text{MD})$$

Thus, we calculated two slightly different BIMC/IIMC formation energies. In addition, we needed to estimate the free energy contribution, which arises from bringing the reactants, acetate

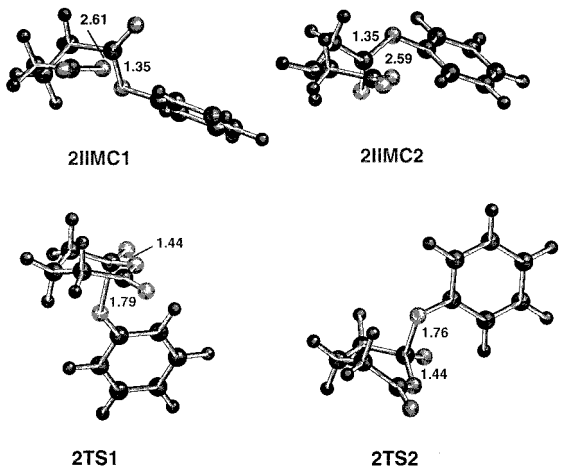

Figure 2. Structures and selected bond distances (in angstroms) of 2IIMC1, 2IIMC2, 2TS1, and 2TS2.

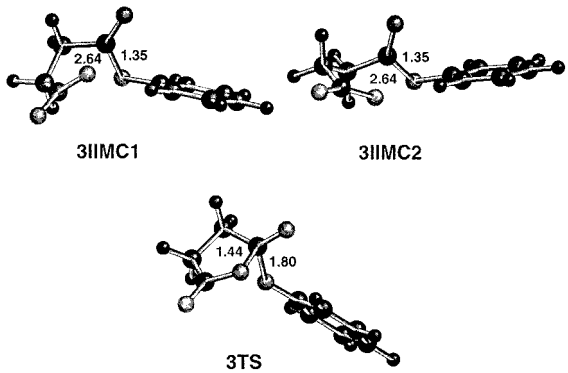

Figure 3. Structures and selected bond distances (in angstroms) of 3IIMC1, 3IIMC2, and 3TS.

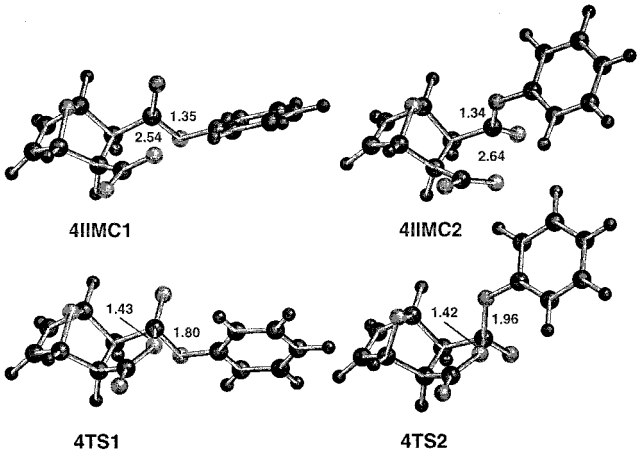

Figure 4. Structures and selected bond distances (in angstroms) of 4IIMC1, 4IIMC2, 4TS1, and 4TS2.

TABLE 1: Relative Energies of the Different Conformations and Transition States of 1 in the Gas Phase (ΔE_{gas}, kcal/mol) and in Solution (ΔE_{sol}((IPCM), ΔE_{sol}(MD)), and Relative Solvation Energies from the Continuum Solvation Model ($\Delta\Delta G_{solv}$(IPCM)) and Explicit Water Simulations ($\Delta\Delta G_{solv}$(MD))

	ΔE_{gas}	$\Delta\Delta G_{solv}$(IPCM)[a]	ΔE_{sol}(IPCM)[b]	$\Delta\Delta G_{solv}$(MD)	ΔE_{sol}(MD)[c]
1TS1	−2.6	22.3	19.7	*d*	17.1
1TS2	3.3	19.1	22.4	*d*	19.8
1BIMC1	−14.4	13.2	−1.2	10.6	−3.8
1BIMC2	−14.2	14.9	0.7	10.6	−3.6
CH_3CO_2- + Ph−C═O(OCH3)	0.0	0.0	0.0	0.0	0.0

[a] IPCM solvation energies were −67.2 and −5.9 kcal/mol for $CH_3CO_2^-$ and Ph−C═O(OCH3), respectively. [b] ΔE_{sol}(IPCM) = ΔE_{gas} + $\Delta\Delta G_{solv}$(IPCM). [c] 1BIMC1 and 1BIMC2: ΔE_{sol}(MD) = ΔE_{gas} + $\Delta\Delta G_{solv}$(MD). 1TS1 and 1TS2: ΔE_{sol}(MD) values of TSs relative to BIMCs are calculated from ΔE_{sol}(IPCM) values. [d] Not calculated.

TABLE 2: Torsion Angles τ1, τ2, and τ3, Relative Solvation Energies (kcal/mol, $\Delta\Delta G_{solv}$((IPCM), $\Delta\Delta G_{solv}$(MD)), and Relative Energies of the Different Conform ations and Transition States of 2 in the Gas Phase (ΔE_{gas}) and in Solution (ΔE_{sol}(IPCM), ΔE_{sol}(MD))

	τ1	τ2	τ3	ΔE_{gas}	$\Delta\Delta G_{solv}$(IPCM)	ΔE_{sol}(IPCM)[a]	$\Delta\Delta G_{solv}$(MD)	ΔE_{sol}(MD)[b]
2TS1	317.8	49.3	54.4	7.8	13.3	21.1	c	17.2
2TS2	55.2	331.8	82.2	8.1	13.1	21.1	*c*	17.2
2IIMC1	300	96.1	216.5	−3.2	9.6	6.3	1.8	−1.4
2IIMC2	293.3	87.5	46.1	−3.0	5.6	2.5	2.2	−0.8
2EX1	175.9	59.2	56.2	−0.5	−6.7[c]	−7.2[d]	1.5	1.0
2EX2	65.4	173.3	63	−1.9	2.5	0.5	2.0	0.1
2EX3	65	173.4	286.3	−1.3	2.6	1.3	1.8	0.5
2EX4	177.8	178.7	71.7	2.0	3.2	5.3	1.7	3.8
2EX5	183.6	181.4	189.9	0.0	0.0	0.0	0.0	0.0
2EX6	64.5	178.4	181.3	−1.7	6.6	4.9	1.5	−0.2
2EX7	65.2	73.8	195.6	−1.1	1.8	0.7	1.2	0.2
2EX8	168.5	62.7	259.3	0.0	1.6	1.5	2.1	2.1
2EX9	68.5	67	46.4	−0.9	5.6	4.7	0.5	−0.5

[a] ΔE_{sol}(IPCM) = ΔE_{gas} + $\Delta\Delta G_{solv}$(IPCM). [b] 2EX1−2EX9: ΔE_{sol}(MD) = ΔE_{gas} + $\Delta\Delta G_{solv}$(MD). 2TS1 and 2TS2: ΔE_{sol}(MD) values of TSs relative to IIMCs are calculated from ΔE_{sol}(IPCM) values. [c] Not calculated. [d] Solvation energies of 2EX1 were excluded from the data analysis.

TABLE 3: Torsion Angles τ1 and τ2, Relative Solvation Energies (kcal/mol, $\Delta\Delta G_{solv}$((IPCM), $\Delta\Delta G_{solv}$(MD)), and Relative Energies of the Different Conformations and Transition States of 3 in the Gas Phase (ΔE_{gas}) and in Solution (ΔE_{sol}(IPCM), ΔE_{sol}(MD))

	τ1	τ2	ΔE_{gas}	$\Delta\Delta G_{solv}$ (IPCM)	ΔE_{sol} (IPCM)[a]	$\Delta\Delta G_{solv}$ (MD)	ΔE_{sol} (MD)[b]
3TS	22.9	71.5	8.9	4.0	12.9	*c*	12.2
3IIMC1	54.5	43.9	−0.3	2.9	2.6	−0.4	−0.7
3IIMC2	299.5	132.9	0.0	0.0	0.0	0.0	0.0
3EX1	182.4	74.3	2.4	1.1	3.6	0.1	2.5
3EX2	170.9	170.2	3.9	2.2	6.1	−0.9	3.0

[a] ΔE_{sol}(IPCM) = ΔE_{gas} + $\Delta\Delta G_{solv}$(IPCM). [b] 3EX1 and 3EX2: ΔE_{sol}(MD) = ΔE_{gas} + $\Delta\Delta G_{solv}$(MD). 3TS: ΔE_{sol}(MD) value of TS relative to IIMCs is calculated from ΔE_{sol}(IPCM) values. [c] Not calculated.

and acetate phenyl ester, together in a reactive geometry of the bimolecular ion−molecule complex (Figure 1, 1BIMC1 and 1BIMC2). This free energy contribution, which mainly originates from changes in rotational and translational degrees of freedom and concentration effects, is also called the cratic free energy.[10−12] Here we have estimated that this energy is in the range of 4−6 kcal/mol (see below for details).

Free energies for formation of transition states from BIMC/IIMCs (step 2) are calculated from the gas-phase energies (ΔE_{gas}) of the transition states and BIMC/IIMC structures and the corresponding solvation energies calculated using the continuum solvation method (ΔG_{solv}(IPCM)). The calculated reaction activation energies ($\Delta E^{\#}_{gas}$, $\Delta G^{\#}_{sol}$(IPCM), and $\Delta G^{\#}_{sol}$-(MD), Table 6) of **1** (intermolecular reaction) are calculated from the energies of the separated reactants and TSs. For **2**−**4** the TS energies are energy differencies between the most stable conformations (extended or IMC) and TSs. In aqueous phase

TABLE 4: Relative Energies of the Different Conformations and Transition States of 4 in the Gas Phase (ΔE_{gas}) and in Solution (ΔE_{sol}(IPCM)) and Relative Solvation Energies ($\Delta\Delta G_{solv}$((IPCM)

	ΔE_{gas}	$\Delta\Delta G_{solv}$(IPCM)	ΔE_{sol}(IPCM)[a]
4TS1	6.5	1.1	7.7
4TS2	15.6	2.4	18.1
4IIMC1	0.3	−0.1	0.2
4IIMC2	0.0	0.0	0.0

[a] ΔE_{sol}(IPCM) = ΔE_{gas} + $\Delta\Delta G_{solv}$(IPCM).

TABLE 5: Free Energy Changes (kcal/mol) for the BIMC and IIMC Formation in Solution Using Continuum Solvation Energies (ΔG_{IMC}(IPCM)) and Solvation Energies from Explicit Water Simulations (ΔG_{IMC}(MD))

molecule	ΔG_{IMC}(IPCM)	ΔG_{IMC}(MD)
1[a]	2.8−4.8	0.2−2.2
2	2.3	−0.4
3	−4.0	−3.2

[a] Values of **1** include the estimated cratic free energy contribution of 4−6 kcal/mol.

extended conformations are the most stable ones for **2**, IIMCs are the most stable conformations for **3**, and, because of its rigid structure, **4** exists only in IIMC structures.

Quantum Mechanical Calculations. All the geometries of the minima and transition states were optimized at the HF/6-31G* level, and the energies were further calculated at the MP2/6-31+G* level (MP2/6-31+G*//HF/6-31G*). The effect of solvation on the relative energies was estimated by using the isodensity surface polarized continuum model (IPCM option of Gaussian) as implemented in Gaussian94.[13−16] A dielectric constant (ϵ) of 78.3 (water) and HF/6-31G* level were used in the solvation calculations. In these calculations the solute cavity

TABLE 6: Calculated Absolute and Relative Transition State Energies (kcal/mol) of 1−4 in the Gas Phase ($\Delta E^{\#}_{gas}$, $\Delta\Delta E^{\#}_{gas}$) and in Solution ($\Delta G^{\#}_{sol}$, $\Delta\Delta G^{\#}_{sol}$), and the Absolute and Relative Experimental[2,3] Transition State Energies ($\Delta G^{\#}$ (exptl), $\Delta\Delta G^{\#}$ (exptl)) in 50/50 (v/v) Water−Dioxane Solution

molecule	$\Delta E^{\#}_{gas}$	$\Delta\Delta E^{\#}_{gas}$	$\Delta G^{\#}_{sol}$[a]	$\Delta\Delta G^{\#}_{sol}$[a]	$\Delta G^{\#}$ (exptl)	$\Delta\Delta G^{\#}$ (exptl)
1	−2.6	−9.1	24.7(22.1)	17.0(14.4)	27.6	10.8
2	11.0	4.5	20.9(18.6)	13.2(10.9)	23.5	6.7
3	9.2	2.7	12.9(12.9)	5.2(5.2)	20.2	3.5
4	6.5	0.0	7.7	0.0	16.9	0.0

[a] Energies calculated using solvation energies from explicit water simulation in estimating the EXT to IIMC (**2** and **3**) and separated reactants to BIMC solvation (**1**) are in parentheses. IPCM continuum solvation values are used otherwise.

CHART 2

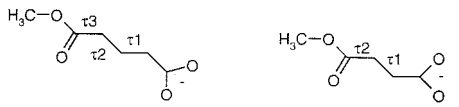

2a **3a**

CHART 3

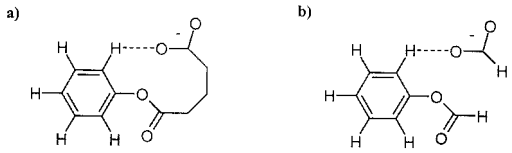

is determined from the electron density of the solute. A value of 0.0004 e/au^3 for the charge density was applied in the determination of the solute boundary. All the ab initio quantum mechanical calculations were performed with Gaussian94 program.[16] The nature of the optimized transition states and selected minima was characterized by vibrational frequency calculations. Frequencies were not used to make thermodynamic corrections to energies since such effects are at least partly included in the relative energies of extended conformations and IMCs calculated with the Boltzman equation (eq 3).

QM Conformational Analyses in the Gas Phase. Since molecules **2** and **3** have a flexible carbon chain and therefore can adopt a number of different conformations we performed conformational analyses for the two molecules. Conformational analyses were done in two stages. First, systematic conformational analyses were done using model compounds of **2** and **3**. In the models, **2a** and **3a** (Chart 2), the phenyl ring of **2** and **3** was replaced by a methyl group. In the case of **2** the torsion angles $\tau1$, $\tau2$, and $\tau3$ were rotated by steps of 60° resulting in total of 27 degenerate pairs (due to symmetry) of initial structures which were geometry optimized at the HF/6-31G* level. In the case of **3** torsion angles $\tau1$ and $\tau2$ were rotated. Detailed results from these calculations are available in the Supporting Information. In the second step of the conformational analyses all the minima found in the first step were used as starting points in the full geometry optimizations of **2** and **3**.

In the IIMCs of **2** and **3** there exists an intramolecular hydrogen bond between the hydrogen of the phenyl ring and the carboxylate oxygen (Chart 3a). Since the hydrogen bond does not exist in the other conformations, the intramolecular basis set superposition error (BSSE) favors the IIMCs relative to the other conformations. The BSSE which is due to the intramolecular hydrogen bond was estimated by calculating the intermolecular BSSE between formate and formate phenyl ester as a model system with the counterpoise procedure (Chart 3b).[17] In the calculations formate and formate phenyl ester were placed in the positions the corresponding groups have in **2** and **3**.

Calculations of the BSSEs were done for the two IIMCs and two extended conformations of both **2** and **3** at the MP2/6-31+G*//HF/6-31G* level. On the basis of these calculations, the BSSE was estimated to favor IIMCs by 3.2 kcal/mol in **2** and 2.9 kcal/mol in **3**. The BSSE for the formation of **1BIMC1** and **1BIMC2** (Figure 1) from the separated reactants was calculated to be 2.9 and 3.3 kcal/mol, respectively. The relative energies of the extended conformations and IIMCs, and the complexation energy of **1** reported include the BSSE correction.

Molecular Dynamical Calculations. The relative solvation energies $\Delta\Delta G_{solv}$(MD) for all the ab initio gas phase conformations of **2** and **3** and for the formation of the bimolecular ion−molecule complex of **1** from the separated reactants acetate and acetate phenyl ester were calculated by carrying out potential of mean force (PMF) calculations. For **2** and **3** the PMF calculations were performed as a function of torsion angles $\tau1$, $\tau2$, and $\tau3$ and for **1** as a function of distance between the carbonyl carbon of acetate phenyl ester and the attacking oxygen of acetate. Values of angles $\tau1$, $\tau2$, and $\tau3$ were taken from the gas-phase geometries, and all the other geometric parameters were free in the PMF calculations. $\Delta\Delta G_{solv}$(MD)s were calculated as a difference between the corresponding PMF calculations in the gas phase and in water. Since $\Delta\Delta G_{solv}$(MD) values of **2** and **3** calculated using this protocol depend on each other we carried out additional simulations, which formed closed cycles between several conformations. These cycles were found to produce solvation energies close to zero confirming that the calculated solvation energies are reliable. In addition, the relative free energy for each perturbation was calculated as the average from forward and reverse simulations. The PMF calculations were done using the thermodynamic integration (TI) method. The water (TIP3P[18]) simulations employed periodic boundary conditions and were run at constant temperature (300K) and pressure (1 atm). A time step of 0.2 fs and SHAKE algorithm[19,20] to constrain all bond distances to their equilibrium values were used. In the case of **2** the solute was placed in a TIP3P water box with dimensions of $\sim25 \times 26 \times 32$ Å^3. In the case of **3** the box size was $\sim24 \times 26 \times 31$ Å^3. In the PMF calculations of **2** and **3** each perturbation from $\lambda = 1$ to $\lambda = 0$ (and from $\lambda = 0$ to $\lambda = 1$) were divided into 201 windows each consisting of 400 steps of equilibrium and 400 steps of production. The total length of one PMF calculation was thus 321ps. In the PMF calculations for the formation of BIMC of **1** the C−O distance was varied in steps of 0.025 Å with 1000 steps of equilibrium and 1000 steps of production. In the gas-phase calculations the distance was varied from 2.7 to 19.0 Å and in water from 2.7 to 9.7 Å. $\Delta\Delta G_{solv}$(MD) was calculated from the energy differences between the ab initio QM gas-phase minimum distance 3.15 Å and the endpoint energies. The size of the water box in these simulations was $\sim35 \times 37 \times 37$ Å^3. Otherwise, the simulation conditions were similar to those used for **1** and **2**.

All the MD calculations were done with the AMBER version 4.1[21] using the Cornell et al. force field[22] and torsional parameters developed in this work for **1**−**3** (See Supporting Information). The atomic charges of **2**, **3**, acetate, and acetate phenyl ester were calculated with the RESP[23] method at the HF/6-31G* level. The charges for **2** and **3** were fit to two conformations of each molecule. In the fit one molecule was in an extended conformation ($\tau1$, $\tau2$, $\tau3 \approx 180°$) and another was IIMC.

Results and Discussion

Geometries and Gas-Phase Energies. Two bimolecular ion−molecule complexes (1BIMC1, 1BIMC2) and two transition states (1TS1, 1TS2) were found for the reaction of acetate with acetate phenyl ester (**1**) corresponding to the anti (1BIMC1 and 1TS1) and syn (1BIMC2 and 1TS2) orientations of the molecules (Figure 1). In the gas phase the complexation energies of 1BIMC1 and 1BIMC2 from the infinitely separated reactants are −14.4 and −14.2 kcal/mol (Table 1, ΔE_{gas}), respectively. 1TS1 has transition state energy of −2.6 kcal/mol (as compared to the isolated reactants), which is 5.9 kcal/mol more favorable than that of 1TS2. 1TS1 is 11.8 kcal/mol higher in energy than 1BIMC1, the most stable of the gas-phase structures of **1**.

Conformational analysis produced 11 different degenerate pairs of conformations for glutarate monoester (**2**). The extended conformations (2EX1-2EX9) of **2** are 1.3−5.2 kcal/mol less stable than 2IIMC1, the more stable of the two IIMCs (Figure 2, Table 2). The structures of the IIMCs differ in the conformation of the carbon chain. In 2IIMC1, which is 0.2 kcal/mol more stable than 2IIMC2, the chain is puckered toward the oxygen of the leaving phenoxide, whereas in 2IIMC2 the chain puckers away from the oxygen. Two TSs, 2TS1 and 2TS2 (Figure 2), were found for the intramolecular reaction of **2**. Again, 2TS1, in which the carbon chain is puckered toward the oxygen, is the more stable (by 0.3 kcal/mol) of the isomeric transition states. The breaking C−O bond is slightly longer (1.794 vs 1.764 Å) in 2TS1 than in 2TS2.

In the case of succinate monoester (**3**) four different degenerate pairs of conformations were found. The two degenerate pairs of the extended conformations are 2.7 (3EX1) and 4.2 kcal/mol (3EX2) less stable than 3IIMC1 (Table 3). In analogy to **2**, the two IIMCs (Figure 3, 3IIMC1, 3IIMC2) differ by the puckering of the carbon chain. 3IIMC1, in which the chain is puckered toward the oxygen of the leaving phenoxide, is 0.3 kcal/mol more stable than 3IIMC2. However, only one transition state, 3TS (Figure 3), was found. In 3TS the breaking C−O bond is 1.797 Å, and the five-membered ring formed in the intramolecular attack is almost planar with slight puckering toward the oxygen of the leaving group (torsion C−C−C−C = 22.9°). Only one TS was found in this case probably because the energy required for the interconversion of the ring conformation of a five-membered ring at the transition state is very low.

Due to the rigid structure 3,6-endoxo-Δ^4-tetrahydrophthalate monoester (**4**) has only two ground-state IIMCs (4IIMC1 and 4IIMC2), and two transition states (Figure 4, Table 4, 4TS1 and 4TS2). Although the IIMCs are within 0.3 kcal/mol in energy, the transition state 4TS1 is 9.1 kcal/mol more favorable than 4TS2. The C−O distance is 1.805 Å in 4TS1 and 1.962 Å in 4TS2. The high energy of 4TS2 is due to the short distance (3.0 Å) between the negative charge bearing oxygen of the leaving phenoxide and the exocyclic oxygen.

In general the optimized geometries of **2**−**4** of this study are close to those calculated earlier at the HF/6-31+G* level.[9] For example, the breaking C−O bonds of the transition states are within 0.03 Å and in IIMCs distances between the attacking oxygen and the carbonyl carbon are within 0.1 Å at the HF/6-31G* and HF/6-31+G* level. However, in the case of **4** a notable difference is observed between the HF/6-31G* results of this study and the earlier HF/6-31+G* results. Two IIMCs were found here for **4**, while only the corresponding tetrahedral intermediates were observed in the earlier calculations at the HF/6-31+G* level. In the tetrahedral intermediate a covalent bond is formed between the nucleophilic oxygen and the ester carbonyl, while there still exists a covalent bond between the carbonyl carbon and the oxygen of the leaving phenoxide. The geometry optimizations of the tetrahedral intermediate at the HF/6-31G* level and IIMC at the HF/6-31+G* showed that both structures exist at the two computational levels. The tetrahedral intermediate was calculated to be 3.1 kcal/mol higher in energy than IIMC at the MP2/6-31+G*//HF/6-31G* level. Thus, the tetrahedral intermediate exists as an intermediate in the reaction.

Solvation Energies from Explicit Water and Continuum Solvation Calculations. The solvation free energy difference ($\Delta\Delta G_{solv}$(MD)) upon the formation of BIMC of **1** from the separated reactants was calculated to be 10.6 kcal/mol (PMF energy for complexation is −7.7 kcal/mol in the gas phase and 2.9 kcal/mol in water) using the explicit water PMF calculations (Table 1, $\Delta\Delta G_{solv}$(MD)). The corresponding energies from the continuum solvation calculations ($\Delta\Delta G_{solv}$(IPCM)) are 13.2 and 14.9 kcal/mol for 1BIMC1 and 1BIMC2, respectively.

A comparison of the relative solvation energies of the various conformations of **2** (Table 2) shows that the energies from the explicit water simulations ($\Delta\Delta G_{solv}$(MD)) are smaller than the energies from the continuum calculations ($\Delta\Delta G_{solv}$(IPCM)). However, the trend that the extended conformations are better solvated than the two IIMCs and that 2EX5 has the most favorable solvation energy is reproduced with both models. A probable reason for the difference in the solvation energies is the fact that in the explicit water simulations, only the three torsion angles were set to the gas phase values and the rest of the molecule was allowed to adapt to the environment. Thus, the structure of the molecule and especially the carboxylate group, which has a large solvation free energy, is solvated well in each conformation. In contrast, in the continuum calculations gas-phase structures were used without allowing the geometries to relax resulting in more unfovarable solvation energies for complex formation. This also applies to the solvation energies of **1** and **3**.

In the case of **3** the MD simulations predict that the extended conformation 3EX2 is the most favorably solvated conformation (Table 3, $\Delta\Delta G_{solv}$(MD)). However, all the $\Delta\Delta G_{solv}$(MD) values are within 1 kcal/mol. In contrast, IPCM calculations predict that 3IIMC1 has the largest solvation energy and that 3EX2 is solvated 2.2 kcal/mol worse than 3IIMC1.

The IPCM model was used to calculate the relative solvation energies between the IMCs and the transition states ($\Delta\Delta G_{solv}$(IPCM), Tables 1−4). In all the cases the transition states are solvated worse than the IMCs. The differences are the largest for **1**. In this case the transition states have ΔG_{solv}(IPCM)s which are 4.2−9.1 kcal/mol smaller than those of BIMCs. In the case of **2** these differences are 3.5−7.7 kcal/mol, in the case of **3** 2.9 and 4.0 kcal/mol, and in the case of **4** 1.2 and 2.5 kcal/mol. Even though there are some inherent uncertainties in the use of the continuum solvation model, i.e., the use of gas-phase geometries, implicit treatment of solvent, and the use of solute cavity, calculated relative solvation energies for the BIMC/IIMC to TS reaction clearly show that the solvent destabilization of the transition states decreases in the series **1** > **2** > **3** > **4**.

Free Energies of Ion−Molecule Complex Formation (Step 1). To compare the calculated reaction energy of **1** with that obtained from experiment, we need to estimate the free energy contribution (cratic free energy[10−12]) which arises from bringing the reactants, acetate and acetate phenyl ester, together in a reactive geometry of the bimolecular ion−molecule complex

(1BIMC1 and 1BIMC2). Here we have estimated that this energy is in the range of 4−6 kcal/mol. These numbers come from our earlier estimate of the cratic free energy contribution to position *N*-methyl acetamide and methanol together in a reactive geometry.[7] This estimate, 4.1−5.4 kcal/mol, was based on MD calculations in explicit water and the use of a recent approach of Hermans and Wang[10] to calculate the cratic free energy. In addition, simple geometric considerations produced a value in the same range. The numbers used are close to 7 kcal/mol calculated for the cratic component of the free energy for binding of benzene in a cavity in a mutant form of T4 lysozyme.[10] It is also in agreement with the earlier estimates for the gain in entropy when an intermolecular reaction is changed to an intramolecular one.[6,24,25] Also, a number in this range has been estimated based on the fusion energies of small molecules[26] and from the data for the binding of ligands to protein receptors.[27] In the latter case the binding free energy gained by covalently linking two moieties into the same ligand was 4−7 kcal/mol. The IMC formation free energy of **1**, which includes the cratic free energy contribution, and of **2**−**4** in solution calculated using the Boltzman equation (eq 3) are reported in Table 5 (ΔG_{IMC}(IPCM) and ΔG_{IMC}(MD)).

For **1** the IMC formation free energies calculated for the more stable BIMC in solution are 2.8−4.8 kcal/mol (Table 5, ΔG_{IMC}-(IPCM)) when the continuum results are used and 0.2−2.2 kcal/mol (ΔG_{IMC}(MD)) when the solvation energies from explicit water simulations are used. Formation of IIMC for **2** is 2.3 kcal/mol endothermic when continuum results and slightly exothermic (−0.4 kcal/mol) when MD results are used. However, in the case of **3**, the IIMC is predicted to be −4.0 kcal/mol (continuum) and −3.2 kcal/mol (MD) more stable than the extended conformations. Interestingly, based on ab initio gas-phase energies and AM1.SM2.1 solvation energies, the IIMC of **2** has been reported to be slightly more stable and the IIMC of **3**, ∼3 kcal/mol more stable the corresponding extended structures,[9] both in agreement with the results of this work. Thus, the extended conformations and IIMC are predicted to be close in energy for **2**. In the case of **3** the IIMC is the most stable conformation in the gas phase and the inclusion of solvation energies either from the continuum or MD calculations does not change the situation. Partial support for the existence of an IIMC structure for **3** in solution can be found from the experimental work of Bruice and Turner.[28] They suggested that the change of the solvent changes the conformation of **3** from "cisoid to transoid". It is also in line with the observation that X-CH_2−CH_2−Y molecules (X and Y are electronegative groups) favor gauche conformations (the "gauche effect") in the gas phase and in solution.[29] For example, the observed conformational preference of succinate monoanion is about 70% gauche.[29,30] Furthermore, measured vicinal NMR proton−proton coupling constants suggest that gauche conformation is the major one for **3** in aqueous solution.[31] Calculations of this work suggest that owing to the favorable intramolecular interactions between the carboxylate group and phenyl ring the gauche preference is larger for succinate monophenyl ester (**1**) than for succinate monoanion.

The probability of formation and the enthalpy of formation of a near-attack conformation (NAC), as obtained from the calculations with the MM3 method, have been suggested to explain quantitatively the reaction rates in the intramolecular anhydride formation reaction.[5] The calculated IMC formation free energies of **1**−**3** (Table 5) of this work are in qualitative agreement with this suggestion: the order of reactivity of **1**−**3** (**1** < **2** < **3**) follows the reverse order of the calculated IMC formation energies. However, the IMC formation energies increase the calculated reaction activation energies of only **1** and **2**. In the case of **3** and **4** the IIMCs are the most stable ground state conformations. In addition to IMC formation energies our calculations suggest (see below) that formation of TSs from IMCs is also responsible for the reactivity differences of **1**−**4**.

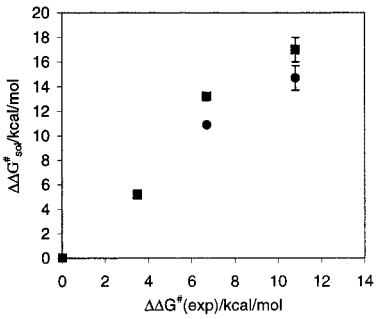

Figure 5. Correlation between the relative experimental ($\Delta\Delta G^{\#}$(exptl), kcal/mol) and the relative calculated TS energies ($\Delta\Delta G^{\#}_{sol}$, kcal/mol). $\Delta\Delta G^{\#}_{sol}$ values of **1**−**4** calculated using continuum solvation energies are drawn with squares and those of **1**−**3** using solvation energies from explicit water simulations with dots. Note that for **3** the calculated energies are the same with both computational methods.

Comparison of the Calculated and Experimental Reaction Energies. The calculated transition state energies in the gas phase ($\Delta E^{\#}_{gas}$) and in aqueous solution ($\Delta G^{\#}_{sol}$) and the experimental TS energies ($\Delta G^{\#}$(exptl)) for the anhydride formation reaction of **1**−**4** are summarized in Table 6. The calculated relative gas-phase TS energies ($\Delta\Delta E^{\#}_{gas}$, MP2/6-31+G*//HF/6-31G*) of **2**−**4** can be seen to follow the experimental order of reactivity in solution ($\Delta\Delta G^{\#}$(exptl)). However, both the calculated absolute and relative numbers are smaller than the corresponding experimental values. The TS energy of **1** is negative because a stable ion-molecule complex is formed in the gas phase. The energy barrier from 1BIMC to 1TS1 is 11.8 kcal/mol (Table 1), only 0.8 kcal/mol larger than the barrier of **2**. The inclusion of solvation energies increases the TS energies both in terms of absolute ($\Delta G^{\#}_{sol}$) as well as the relative ($\Delta\Delta G^{\#}_{sol}$) numbers. The increase is the largest for **1**, which has also an unfavorable solvation and cratic free energy contribution for the formation of BIMC from the separated reactants.

Figure 5 shows almost linear correlation between the relative calculated aqueous phase ($\Delta\Delta G^{\#}_{sol}$) and relative experimental ($\Delta\Delta G^{\#}$(exptl)) TS energies of **1**−**4**. The correlation equations are $\Delta\Delta G$(exptl) = 0.585DDE$_{sol}$ + 0.042 (r^2 = 0.972, IPCM solvation energies), and $\Delta\Delta G$(exptl) = 0.718DDE$_{sol}$ − 0.225 (r^2 = 0.979, MD solvation energies.) It must be noted that the correlation between the experimental and calculated numbers is not quantitative (slope is not 1) and that the calculated absolute TS energies in Table 6 are clearly smaller than the experimental numbers. These differences can be due to a number of reasons. First, the experimental values are for the compounds which have *para* bromo substituted phenyl rings and the experiments were carried out in 50/50 (v/v) water−dioxane solution.[2,3] Instead, in this work we used compounds which have bromine replaced by hydrogen and water as a solvent. It is known experimentally that both these changes decrease the reaction rate of anhydride formation. This consideration, however, would tend to increase the discrepancy between the absolute reaction activation energies. Second, additional differences can originate from the modeling of the transition states of the solution reaction.[13,32,33] Here we used gas-phase geometries and continuum solvation

SCHEME 1

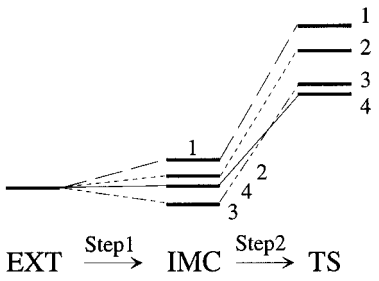

model in estimating the solvation energies for the IMC to TS transformation. Since the solvation energies depend on the cavity radius and dielectric constant changes in these parameters would have changed the solvation energies as well. As can be seen from Table 6 the solvation free energies contribute in an important way to the TS energy differences. Additional solvation energy calculations at the MP2 level and with larger basis sets were found to decrease both the absolute and relative solvation energies (data not shown). This suggests that correlation between the calculated and experimental values would be more quantitative if higher level calculations were used in solvation calculations. It must be noted that hybrid QM/MM calculations or geometry optimizations with continuum solvation model could be used to include the effects of solvent on the geometries and energies of the ground and transition states. However, because of the large number of conformations considered in this study we decided to use computationally less expensive approaches. Third, the ab initio quantum mechanical levels used (MP2/6-31+G*//HF/6-31G* and HF/6-31G*-(IPCM)) are not high enough that quantitative results could be expected. However, since the correlation between the experimental and calculated numbers is very good, we think that the major factors affecting the reactivities of **1**−**4** are modeled reliably enough allowing us to use the results in explaining the differences in the reactivities of the molecules.

The differences in the gas-phase energies, solvation energies, and the cratic free energy contributions were all found to be important in explaining the reactivity differences of **1**−**4**. However, depending on the molecule, the relative importance of the contributions were found to be different. On the basis of the calculated IMC formation and reaction activation free energies in solution we constructed a semiquantitative reaction scheme (Scheme 1) depicting the origin of the relative differences in the rates of the anhydride formation of **1**−**4**.

For **1** the formation of BIMC from separated reactants is the step (step 1) which is mainly responsible for its lower reactivity compared to intramolecular reactions of **2**−**4**. Unfavorable BIMC formation energy of **1** is due to the loss of translational and rotational freedom (cratic free energy) and solvation effects. For **1** the formation of TS from BIMC (step 2) further decreases the relative reaction but to a lesser extend than step 1. Formation of IIMC is slightly unfavorable for **2**, whereas IIMC is the most favorable ground state conformation for **3** and the structurally rigid **4**. Thus, for **2**−**4** it is the IIMC to TS part of the reaction (step 2) which, for the most part, determines the relative reactivities of the molecules. These differences originate from the gas-phase and solvation energies of step 2.

Conclusions

In this paper we have studied the intermolecular anhydride formation reaction between acetate and acetate phenyl ester (**1**), and the corresponding intramolecular reaction of glutarate (**2**), succinate (**3**), and 3,6-endoxo-Δ^4-tetrahydrophthalate monoester (**4**) theoretically using ab initio quantum mechanical (QM) gas phase (MP2/6-31+G*//HF/6-31G*), ab initio QM continuum solvation model (IPCM-HF/6-31G*) and molecular dynamical calculations. In this series of compounds the rate enhancement achieved by changing an intermolecular reaction of **1** to an intramolecular reaction of structurally rigid **4** is 10^8. The calculated transition state (TS) energies for the anhydride formation reaction in the aqueous phase correlated well with the corresponding experimental energies.

A significant part of the rate enhancement of changing an intermolecular reaction of **1** to an intramolecular one (**2**−**4**) is due to decrease in rotational and translational freedom. It was estimated here that the free energy contribution which arises from bringing the reactants, acetate and acetate phenyl ester, together in a reactive geometry of complex **1** (the cratic free energy) is 4−6 kcal/mol. The anhydride formation reaction can be divided into two sequential steps: (1) the formation of a ground-state bimolecular ion−molecule complex from separated reactants or intramolecular ion−molecule complex from a pool of extended conformations and (2) the formation of transition state from ion−molecule complex. The gas phase and solvation energies of the both steps are important in determining the relative reaction rates of the anhydrate formation of **1**−**4**. However, depending on the compound the relative importance of the steps and the energy contributions are different.

Bruice et al.[5,9] have studied intramolecular anhydride formation reaction of the molecules similar to the ones studied in this work using partly different computational methods and approaches. Especially because they used near-attack conformations (NAC) and we intramolecular ion−molecule (IIMC) complexes as intermediates in the reaction mechanism (reaction 1, Scheme 1), the direct comparison of the results is not straightforward. However, the following two main conclusions can be drawn from the comparison of the two works. First, the results of both studies showed that the ease of formation of the reactive conformations (NAC or IIMC) has direct effect on the rate of intramolecular reactions. Second, whereas Bruice et al. concluded that the step from NAC to transition state (TS) has no effect on the relative reaction rates of different anhydrides, our calculations show that also this step (from IIMC to TS) affects the reaction rates and that for **2**−**4** both steps have parallel effects on the relative rates.

Acknowledgment. M.P. gratefully acknowledges the support from the Academy of Finland. P.A.K. is grateful to the NIH for support (GM-29072).

Supporting Information Available: Results from the ab initio quantum mechanical conformational analyses of **2a**, **2**, **3a**, and **3**, energies from the potential of mean force calculations of **2** and **3**, and the RESP charges and torsional parameters of **1**, **2**, and **3**. Supporting Information is available free of charge via the Internet at http://pubs.acs.org.

References and Notes

(1) Menger, F. M. *Acc. Chem. Res.* **1993**, *26*, 206−212.
(2) Bruice, T. C.; Pandit, U. K. *Proc. Natl. Acad. Sci. U.S.A.* **1960**, *46*, 402−404.
(3) Bruice, T. C. *Annu. Rev. Biochem.* **1976**, *45*, 331−373.
(4) Menger, F. M. Organic reactivity and geometric disposition. In *Advances in Molecular Modeling*; Liotta, D., Ed.; Jai Press, Ltd.: Greenwich, 1988; Vol. 1, pp 189−213.
(5) Lightstone, F. C.; Bruice, T. C. *J. Am. Chem. Soc.* **1996**, *118*, 2595−2605 and references therein.
(6) Page, M. I.; Jencks, W. P. *Proc. Natl. Acad. Sci. U.S.A.* **1971**, *68*, 1678−1683.

(7) Stanton, R. V.; Peräkylä, M.; Bakowies, D.; Kollman, P. *J. Am. Chem. Soc.* **1998**, *120*, 3448−3457.
(8) Jung, M. E.; Gervay, J. *J. Am. Chem. Soc.* **1991**, *113*, 224−232.
(9) Lightstone, F. C.; Bruice, T. C. *J. Am. Chem. Soc.* **1997**, *119*, 9103−9113.
(10) Hermans, J.; Wang, L. *J. Am. Chem. Soc.* **1997**, *119*, 2707−2714.
(11) Finkelstein, A. V.; Janin, J. *Protein Eng.* **1989**, *3*, 1−3.
(12) Janin, J. *Proteins* **1996**, *24*, i−ii.
(13) Tomasi, J.; Persico, M. *Chem. Rev.* **1994**, *94*, 2027−2094.
(14) Miertus, S.; Scrocco, E.; Tomasi, J. *Chem. Phys.* **1981**, *55*, 117−129.
(15) Wiberg, K. B.; Rablen, P. R.; Rush, D. J.; Keith, T. A. *J. Am. Chem. Soc.* **1995**, *117*, 4261−4270.
(16) Frisch, M. J.; Trucks, G. W.; Schlegel, H. B.; Gill, P. M. W.; Johnson, B. G.; Robb, M. A.; Cheeseman, J. R.; Keith, T. A.; Peterson, G. A.; Montgomery, J. A.; Rachavachari, K.; Al-Laham, M. A.; Zakrzewski, V. G.; Ortiz, J. V.; Foresman, J. B.; Cioslowski, J.; Stefanov, B. B.; Nanayakkara, A.; Challacombe, M.; Peng, C. Y.; Ayala, P. Y.; Chen, W.; Wong, M. W.; Andres, J. L.; Replogle, E. S.; Gomperts, R.; Martin, R. L.; Fox, D. J.; Binkley, J. S.; Defrees, D. J.; Baker, J.; Stewart, J. J. P.; Head-Gordon, M.; Gonzales, C.; Pople, J. A.*Gaussian 94, Revision B.3.*; Gaussian, Inc.; Pittsburgh, PA, 1995.
(17) Boys, S. F., Bernardi, F. *Mol. Phys.* **1970**, *19*, 553−562.
(18) Jorgensen, W. J.; Chandrasekhar, J.; Madura, J. D.; Impley, R. W.; Klein, M. L. *J. Chem. Phys.* **1983**, *79*, 926−935.
(19) van Gunsteren, W. F.; Berendsen, H. J. C. *Mol. Phys.* **1977**, 1311−1327.
(20) Ryckaert, J. P.; Ciccotti, G.; Berendsen, H. J. C. *J. Chem. Phys.* **1977**, *23*, 327−341.
(21) Pearlman, D. A.; Case, D. A.; Caldwell, J. W.; Ross, W. S.; Cheatham, T. E., III.; Ferguson, D. M.; Seibel, G. L.; Singh, U. C.; Weiner, P. K.; Kollman, P. A. AMBER 4. 1; University of California, San Francisco, 1995.
(22) Cornell, W. D.; Cieplak, P.; Bayly, C. I.; Gould, I. R.; Merz, K. M., Jr.; Ferguson, D. M.; Spellmeyer, D. C.; Fox, T.; Caldwell, J. W.; Kollman, P. *J. Am. Chem. Soc.* **1995**, *117*, 5179−5197.
(23) Bayly, C. I.; Cieplak, P.; Cornell, W. D.; Kollman, P. A. *J. Phys. Chem.* **1993**, *97*, 10269−10280.
(24) Genick, U. K.; Devanathan, S.; Meyer, T. E.; Canestrelli, I. L.; Williams, E.; Cusanovich, M. A.; Tollin, G.; Getzoff, E. D. *Biochemistry* **1997**, *36*, 8−14.
(25) Baca, M.; Borgstahl, G. E. O.; Boissinot, M.; Burke, P. M.; Williams, D. R.; Slater, K. A.; Getzoff, E. D. *Biochemistry* **1994**, *33*, 14369−14377.
(26) Searle, M. S.; Williams, D. H. *J. Am. Chem. Soc.* **1992**, *114*, 4, 10690−10697.
(27) Jencks, W. P. *Proc. Natl. Acad. Sci. U.S.A.* **1981**, *78*, 4046−4050.
(28) Bruice, T. C.; Turner, A. *J. Am. Chem. Soc.* **1970**, *92*, 3422−3428.
(29) Price, D. J., Roberts, J. D., Jorgensen, W. L. *J. Am. Chem. Soc.* **1998**, *120*, 9672−9679.
(30) Lit, E. S., Mallon, F. K., Tsai, H. Y., Roberts, J. D. *J. Am. Chem. Soc.* **1993**, *115*, 9563−9567.
(31) Laatikainen, R., Vepsäläinen, J., Peräkylä, M. Work in progress.
(32) Orozco, M.; Luque, F. J.; Habibollah-Zadeh, D.; Gao, J. *J. Chem. Phys.* **1995**, *102*, 6145−6152.
(33) Lim, D.; Jorgensen, W. L. *J. Phys. Chem.* **1996**, *100*, 17490−17500.